

MICROCOPY RESOLUTION TEST CHART
NATIONAL BUREAU OF STANDARDS 1963-A

2

AD-A152 399



Kirchhoff Modeling via Wave Equation Datuming

by

Michael Sullivan

Partially Supported by the Consortium Project of the Center for Wave Phenomena and by the Selected Research Opportunities Program of the Office of Naval Research

Colorado School of Mines

Golden, Colorado 80401

Center for Wave Phenomena
Department of Mathematics
303/273-3557

DTIC FILE COPY

DTIC
SELECTED
APR 15 1985
S A D

This document has been approved for public release and sale; its distribution is unlimited.



85 03 22 034

2

GWP-017



Kirchhoff Modeling via Wave Equation Datuming

by

Michael Sullivan

**Partially Supported by the Consortium Project of the
Center for Wave Phenomena and by the Selected Research
Opportunities Program of the Office of Naval Research**

**Center for Wave Phenomena
Department of Mathematics
Colorado School of Mines
Golden, Colorado 80401
Phone: (303) 273-3557**

**DTIC
ELECTE
S APR 15 1985 D
A**

This document has been approved
for public release and sale; its
distribution is unlimited.

Abstract

The acoustic wavefield reflection response of a plane wave on a cylindrical surface is calculated from a specialization of the Kirchhoff integral. Computational advantages are obtained by assuming that structural changes occur only along the direction of data collection. Off-line geologic invariance permits an integral to be replaced by a short convolution operator. The restriction to single interface modeling permits implementation on personal computers. Also, the single layer algorithm provides the framework for a multi-layer code.

Accession For	
NTIS	
NTIS	
NTIS	
NTIS	
NTIS	
By	
Distribution	
Avail	Res
Dist	

A-1



TABLE OF CONTENTS

INTRODUCTION.....	1
WAVE EQUATION DATUMING.....	3
ALGOITHM DERIVATION.....	5
IMPLEMENTATION.....	9
EXAMPLES.....	12
ACKNOWLEDGEMENTS.....	13
REFERENCES.....	14
FIGURES.....	15

Introduction.

An efficient program has been developed to model the 2-dimensional Kirchhoff acoustic wavefield reflection response of a plane wave on a cylindrical surface. Intuitively, a source function is placed on each differential surface element, and an exploding reflector simulation is performed by initiating all of the sources concurrently. The method discussed here is based on a technique by John R. Berryhill (1979) in which cylindrical symmetry allows for considerable execution time reduction in computing the Rayleigh II integral. In brief, assuming invariance of geologic structure in the off-line direction permits a short convolution operator to replace one of the two requisite surface integrals.

There is an advantage in having a program specialized to single-layer modeling in that the normal-incidence wavefield effects of a plane wave on buried anticlines, synclines, or arbitrary structures may be simulated without the computational overhead associated with performing single-layer responses via a multi-layer program. The small memory requirements and relatively low amount of input/output make the program particularly friendly to implementation on a personal computer (80 traces in 10 minutes on an IBM PC/XT with an 8087 co-processor). Also, the single layer modeling routine is, hopefully, a large step toward developing a multi-layer code.

A general description of the Berryhill technique as applied to wave equation datuming is given. For completeness, a derivation of the algorithm is included. Example simulations are then provided which demonstrate the wavefield effects inherent in the method.

Wave Equation Datuming

The primary application of the extrapolation method employed by Berryhill (1979) is in wave equation datuming. This procedure redefines the surface on which the data are taken, for the purpose of minimizing distortive surface effects. A common example includes downward continuing marine data to an irregular ocean bottom, and then upward continuing the data to a flat plane, using the velocity from under the ocean bottom. This removes the effect that an irregular surface has on deeper reflectors.

In a modeling sense, a source is placed on a cylindrical surface and the resulting wavefield is recorded at another surface. Note that only an inter-datum velocity is required. The technique is therefore based on the "exploding reflector" model of the subsurface using a velocity equal to half the true velocity in order to produce correct arrival times.

In a multi-layer setting, the initial exploding reflector corresponds to the deepest horizon, with an identical source placed on each differential surface element. The resulting wavefield is then recorded at the next reflecting surface. A time section displaying the wavefield as seen by the upper surface is thus produced. To each trace in this time section, the original source function, weighted by a reflection coefficient, is added. When this datum explodes, it extrapolates the effects of the lower reflector, true to Snell's law, as well as extrapolating its own exploding datum upwards. The same procedure is applied to each reflector, as the

wavefield moves toward the earth's surface. Multiples can be included in this method by extrapolating back down to a datum, and then continuing the data upwards.

Algorithm Derivation

The Berryhill algorithm is an application of the Rayleigh II specialization of the Kirchhoff integral. The following outline of the Rayleigh II integral derivation is from Berkhout (1982). Further details can be found in texts by Born and Wolf (1983), and Lipson and Lipson (1981).

Define P as the pressure inside a region, bounded by a surface S , due to a compressional source exterior to S . The free-space Green's function, G , represents a pressure due to an interior source. Therefore

$$(\nabla^2 + K^2) P = 0 \quad ,$$

$$(\nabla^2 + K^2) G = -4\pi\delta(x-x_a)\delta(y-y_a)\delta(z-z_a) \quad ,$$

$$\text{and} \quad G = \frac{e^{-jkr}}{r} \quad .$$

Applying Green's theorem results in

$$\oint_S (PVG - GVP) \cdot \vec{n} \, ds = -4\pi P(x_a, y_a, z_a) = -4\pi P_a$$

Noting that

$$-\frac{\partial P}{\partial n} = \rho_0 \frac{\partial V_n}{\partial t} ,$$

where ρ_0 is the static density and V_n is the normal component of particle velocity leads to the Kirchhoff integral,

$$P_a = \frac{1}{4\pi} \int_S \left[\frac{P(1+jkr)}{r^2} \cos\phi e^{-jkr} + j\omega \rho_0 V_n \frac{e^{-jkr}}{r} \right] ds .$$

Where \hat{n} is now defined as the inward pointing normal, and

$$\cos\phi = -\frac{\partial r}{\partial \hat{n}}$$

The Kirchhoff integral states that the pressure at a point A is a surface extrapolation of monopole normal velocity components, and a dipole pressure field.

The surface is chosen to be a closed hemisphere, such that the distance between the point A and the planar portion of the hemisphere is much less than the distance between the point A and the acurate portion. The integration surface is therefore the planar base of a very large hemisphere.

An alternate (negative image) Green's function eliminates the normal velocity component term, providing the Rayleigh II integral.

$$P_a = \frac{1}{2\pi} \int_S P \frac{1+jkr}{r^3} \cos\phi e^{-jkr} ds .$$

It is interesting to note that applying

$$-\frac{\partial P}{\partial n} = \rho_0 \frac{\partial V_n}{\partial t}$$

to the Rayleigh I integral produces the Rayleigh II integral, with P replaced by V_n . Thus, the Rayleigh II integral can be seen as a means of forward (or reverse) extrapolation of either a dipole pressure field, or the normal components of particle velocity.

Berryhill (1979) starts with the time domain representation of the Rayleigh II integral, and then assumes that there is no variance of the extrapolated surface in the y-direction. Under this assumption, and in Berryhill's notation,

$$u(0, z, t) = \frac{1}{2\pi} \int_{-\infty}^{\infty} dx z \int_{-\infty}^{\infty} dy \frac{1}{r^3} \left[u(x, 0, t-r/c) + \frac{r}{c} \frac{\partial}{\partial t} u(x, 0, t-r/c) \right] ,$$

where the geometry is defined in Figure 1.

The y-integration is replaced with a convolution, leading to

$$u(o, z, t) = \frac{1}{\pi} \int_{-\infty}^{\infty} dx \frac{c}{cr_x} \frac{du(x, o, t)}{dt} * H(t - r_x/c) \frac{d \tan \varphi}{dt} ,$$

where $H(t)$ is the unit step function, and

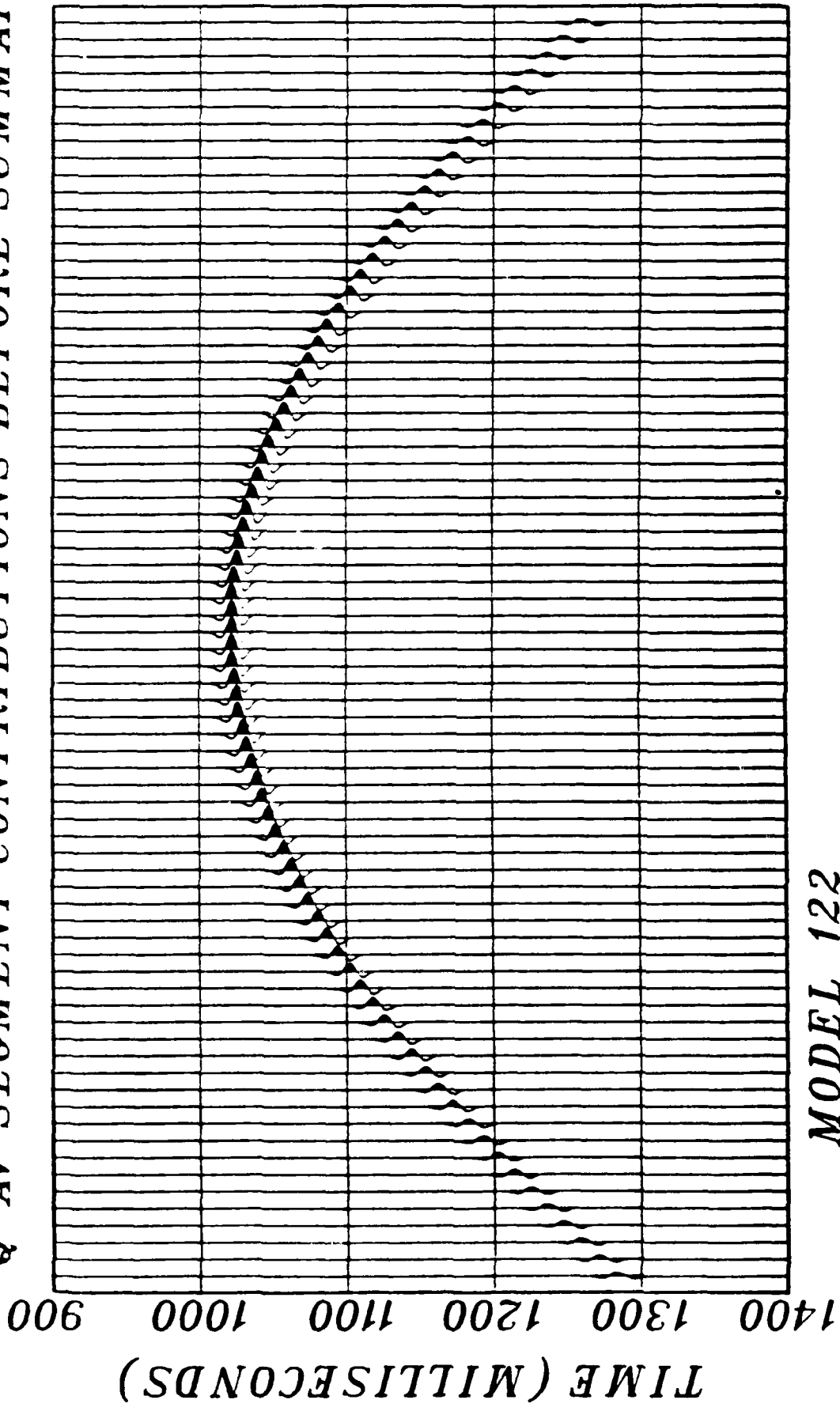
$$\frac{d \tan \varphi}{dt} = \frac{c}{r_x} \frac{t}{(t^2 - r_x^2/c^2)^{1/2}} .$$

In the digital implementation of the algorithm, the derivative on the source, $u(x, o, t)$, is moved to the tangent operator.

This new tangent operator, containing the off-line integral contributions, goes to zero rapidly. Typically, the first 9 points of the operator do nicely, for computer results, as seen in Figure 2. Therefore, the response at a point due to a wavefield defined on a surface is a sum of line responses on the surface. A single line response is illustrated in Figure 3. Each line response is thus obtained by convolving the surface source function with a short off-line operator.

A final assumption is made in defining a curved surface as a sequence of properly weighted planar segments. The diffraction response due to segment corners is negligible if the associated dihedral angles are less than a few degrees.

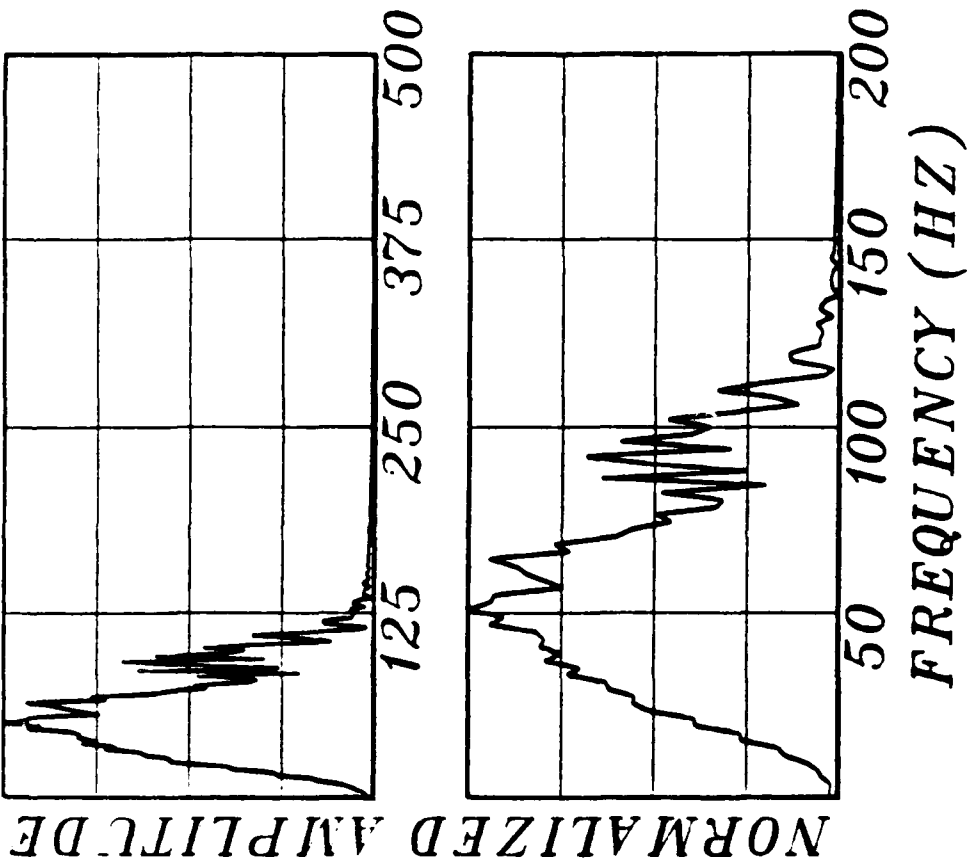
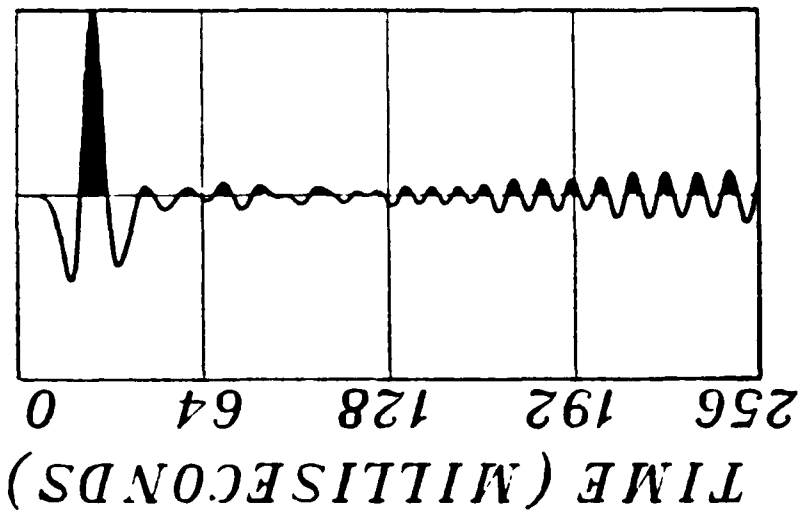
Q-AV SEGMENT CONTRIBUTIONS BEFORE SUMMATION



MODEL 122

FIGURE 7

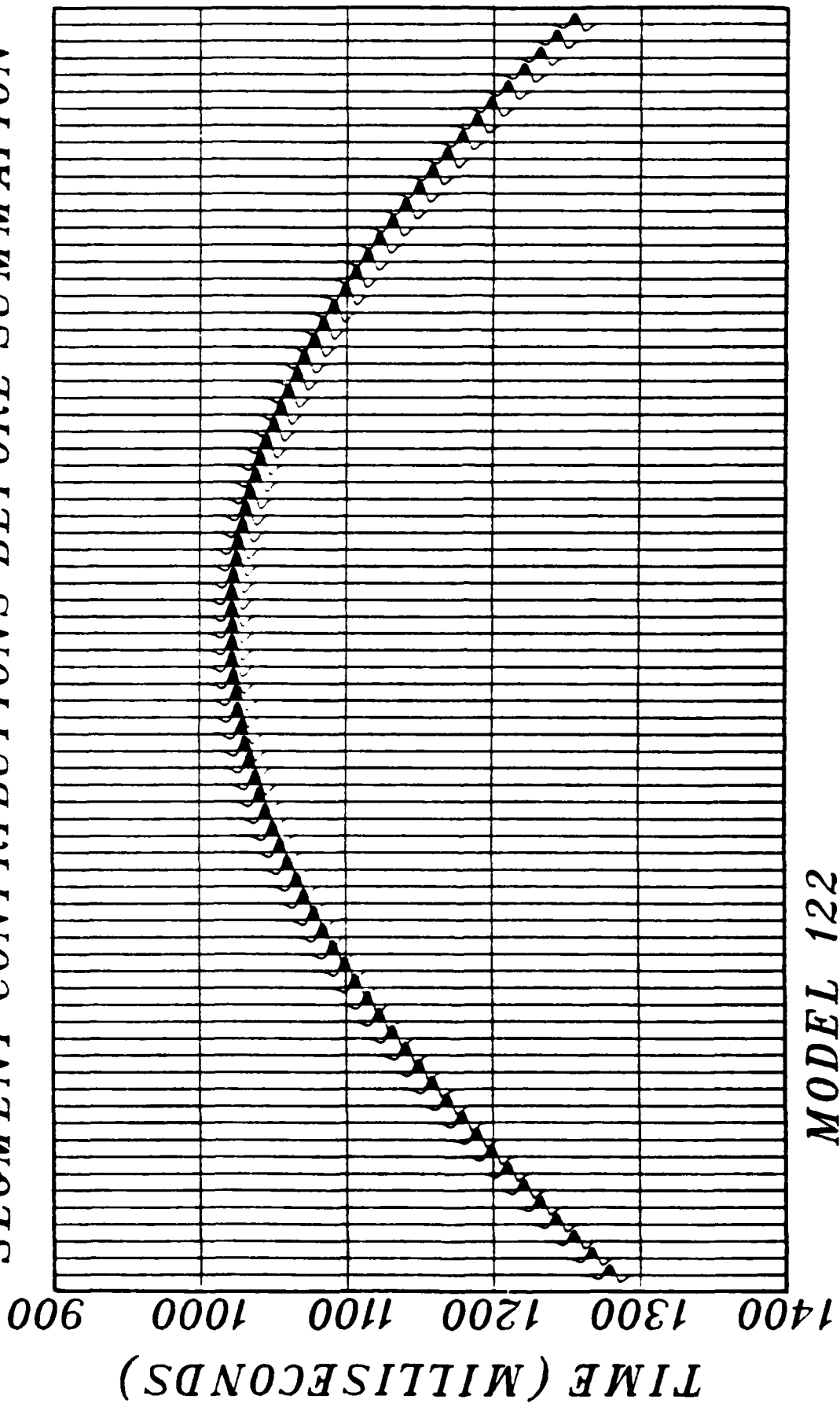
KIRCHHOF
WAVELET



MODEL 122

FIGURE 6

SEGMENT CONTRIBUTIONS BEFORE SUMMATION



MODEL 122

FIGURE 5

KIRCHHOFF INTEGRATION SEGMENTS

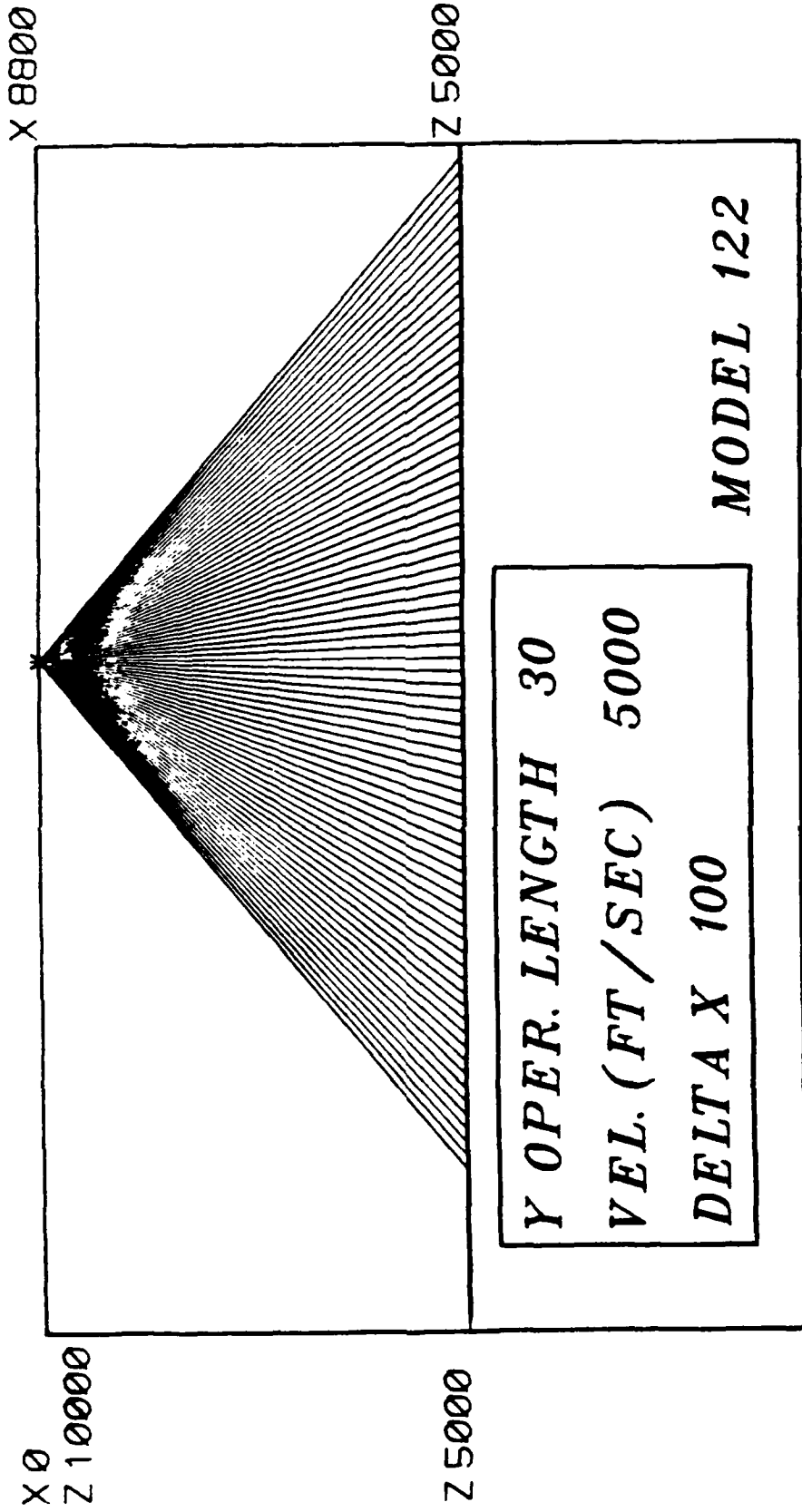
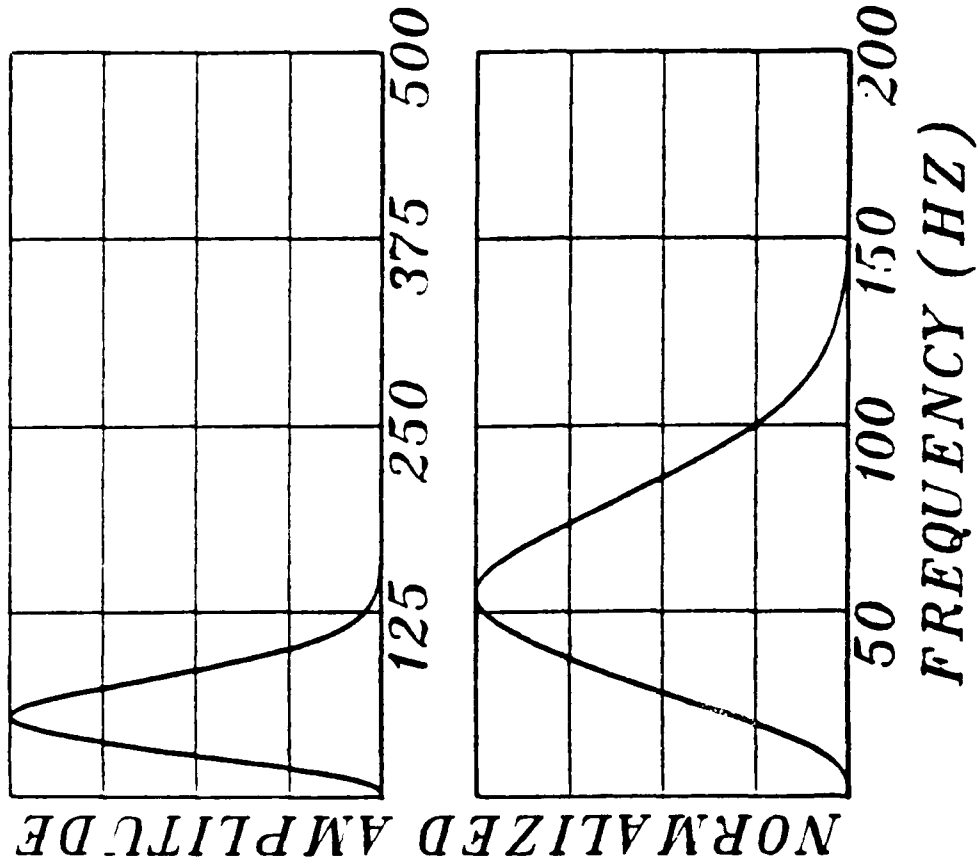
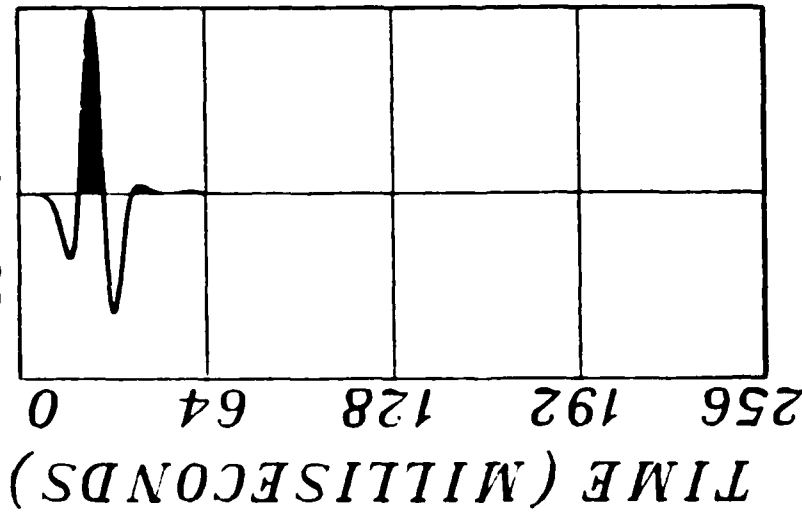


FIGURE 4

**KIRCHHOFF
WAVELET**



MODEL 121

FIGURE 3

CONVOLUTION OPERATOR FOR Y-INTEGRATION

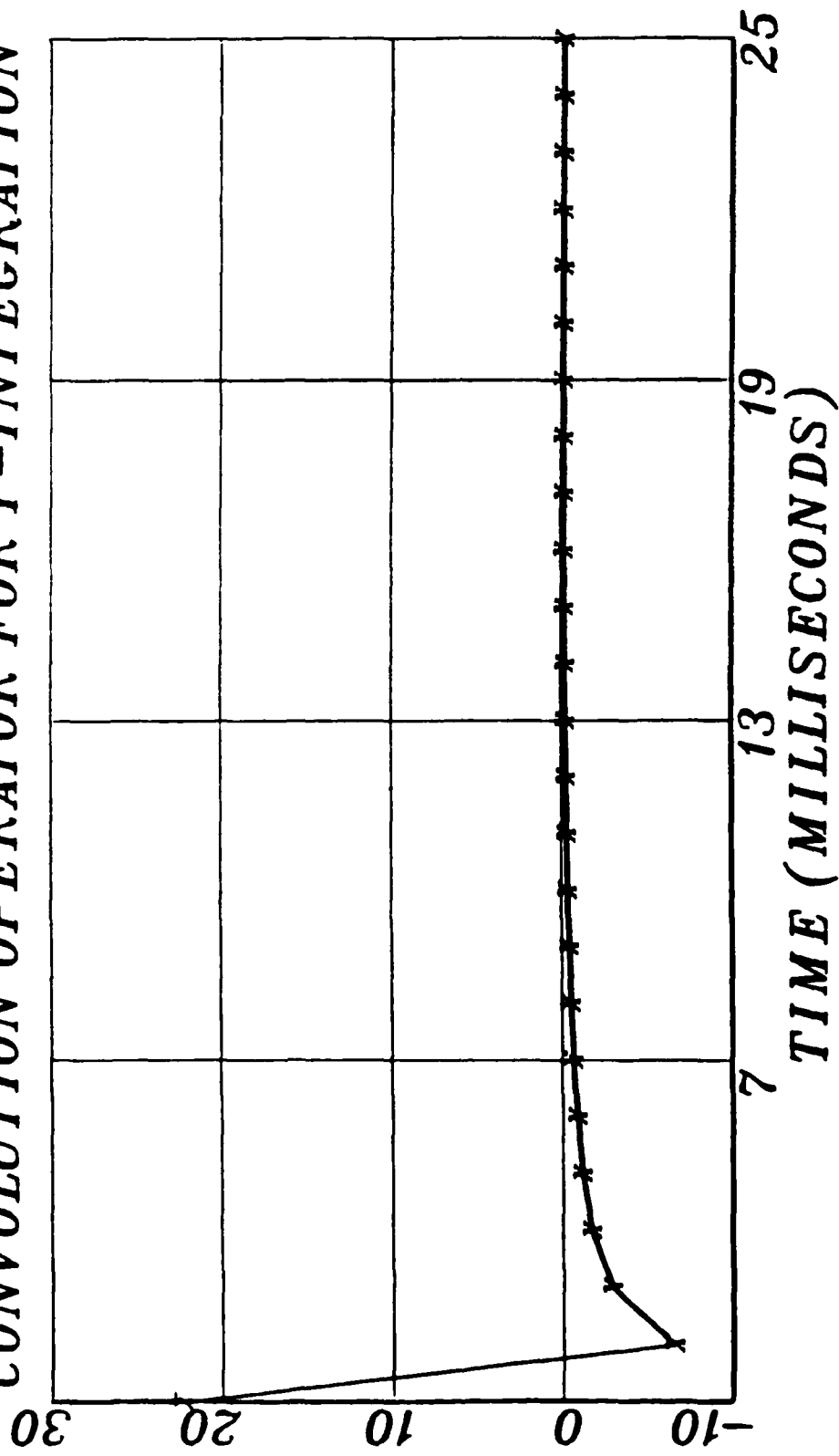


FIGURE 2

$$U(x, z, t) = \frac{1}{2\pi} \int_0^\infty \int_0^\infty U(x, \theta, T-R/C) \\ + R/C \frac{2}{2T} U(x, \theta, T-R/C)]$$

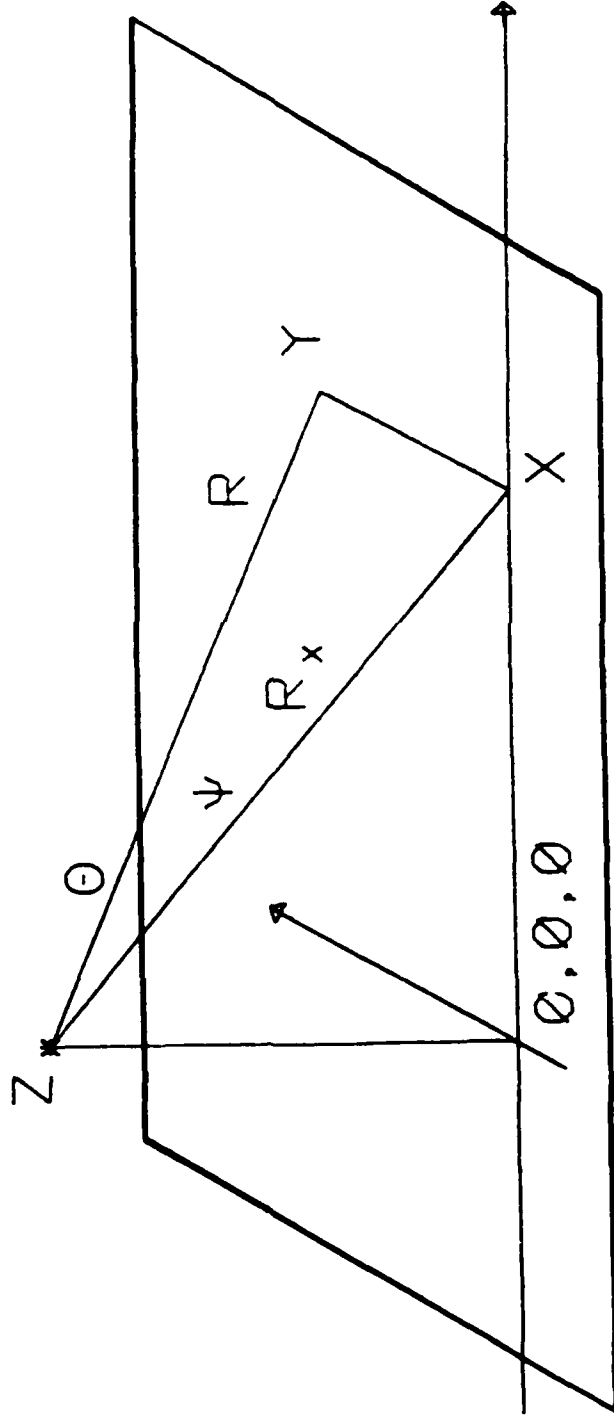
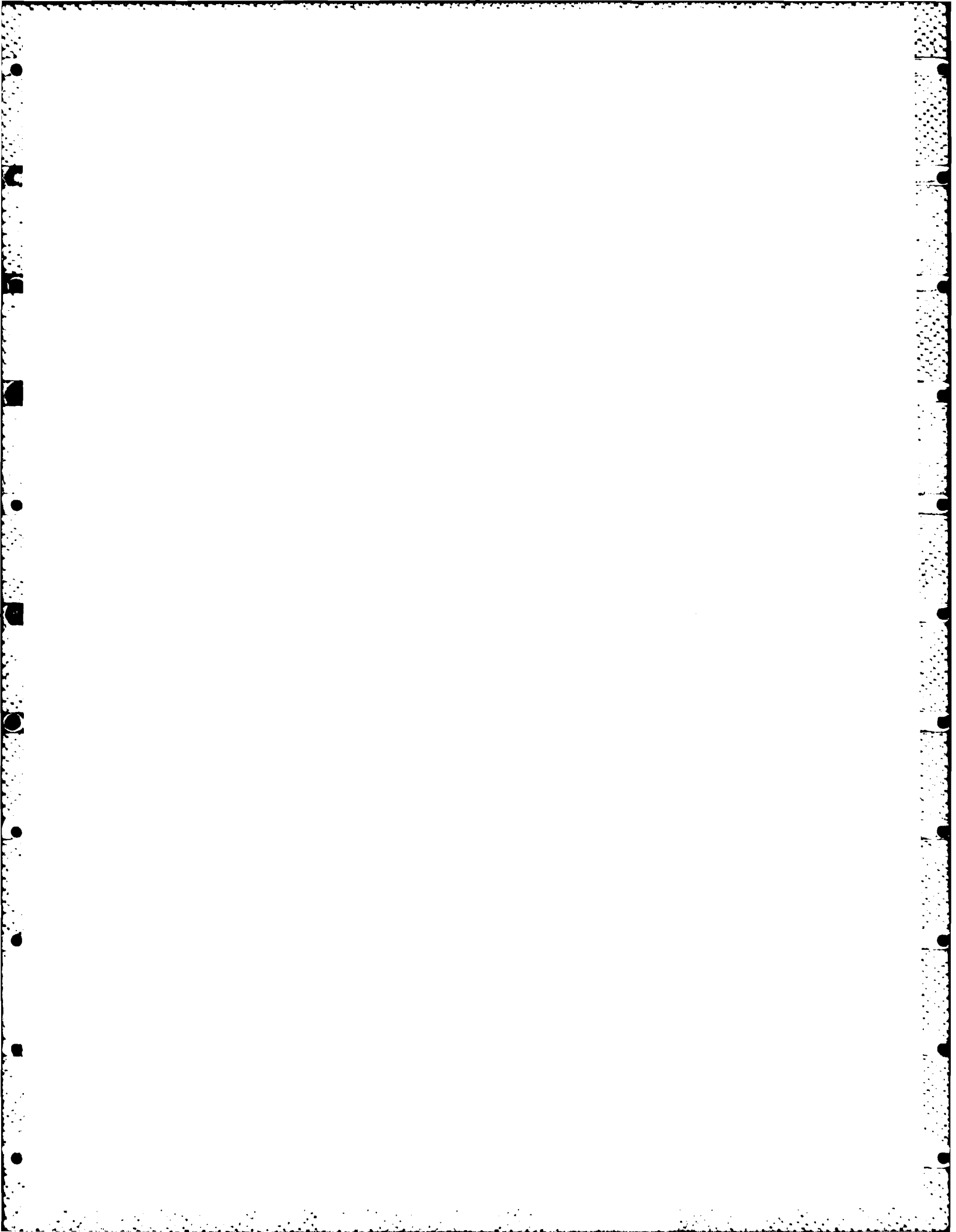


FIGURE 1
FOLLOWING BERRYHILL [1979]

References

- Berkhout, A.J., 1982, Seismic Migration - Imaging of Acoustical Energy by Wave Field Extrapolation. - A. Theoretical Aspects: Elsevier Scientific Publishing Company.
- Berryhill, J.R., 1979, Wave Equation Datuming: Geophysics, v. 44, p. 1329-1344.
- Born, M., and Wolf, E., 1983, Principles of Optics - Electromagnetic Theory of Propagation Interference and Diffraction of Light: Oxford, Pergamon Press.
- Lipson, S.G., and Lipson, H., 1981, Optical Physics: Cambridge, Cambridge University Press.



kept constant, with the height of the feature increasing. The diffraction energy in the corresponding time sections illustrates the fidelity of the method of producing wavefield responses.

Acknowledgements

The author gratefully acknowledges the support of the Office of Naval Research, Mathematics Division, through its Selected Research Opportunity Program, and the Consortium Project on Seismic Inverse Methods for Complex Structures at the Center for Wave Phenomena, Colorado School of Mines. Consortium members are Amoco Production Company, Conoco, Inc., Geophysical Exploration Company of Norway A/S, Golden Geophysical Corp., Marathon Oil Company, Mobil Research and Development Corp., Phillips Petroleum Company, Sun Exploration Research, Texaco USA, Union Oil Company of California, and Western Geophysical.

Examples

All of the examples in Figures 10-17 were generated using the flat-topped averaging operator. The out of plane operator lengths used were extravagantly long, and computationally wasteful. A maximum of 10 points works just as well; (do as I say, and not as I do!). Receivers are on a flat datum, but need not necessarily be so. A cubic spline is fit to both the receiver and reflector surfaces. The two lines drawn to the exploding surface from each receiver depicts the boundaries of the respective integration zones.

A search is conducted for spectral points associated with each receiver. The search zone is symmetric about the receiver, and 8 Fresnel zones wide. The location of an extreme right and an extreme left spectral point delineate the integration zone, the outer borders of which are one Fresnel zone beyond each spectral point. If no spectral point is found, the integration is performed in a zone directly under the receiver.

Figure 10 illustrates the geometry of a syncline model. Receivers are positioned along the top of the diagram, with their respective integration zones delineated. The resultant time section in Figure 11 depicts the "bow tie" effect associated with synclinal structures. Note that the waveform appearing in the center of the bow tie is the derivative of the Ricker source function. This is due to the buried focus.

Figure 12 through 17 model the diffraction effects of an anticline. The distance between the receiver datum and the base of each structure is

increment is a function of a maximum frequency.

frequency domain aliasing is displayed via a standard scale and a zoom plot.

The averaging operator permits a constant sample rate along the integration surface by filtering out the high frequency components of the late arrivals. This is accomplished by convolving each segment response with a flat-topped averaging operator. The length of the operator being proportional to the difference in arrival times of adjacent segments. Figure 7 displays the individual segment contributions after application of the averaging operator. Note that the frequency content of the late arrivals has been reduced. Summation of the line sources results in a much cleaner wavelet, as displayed in Figure 8.

The source function in all examples is a causal Ricker wavelet. As depicted in Figure 9, it is symmetric in the time domain, consisting of a small trough, a large peak, and a small trough. In the frequency domain, the wavelet is approximately Gaussian shaped, with "important" information coming from frequencies of up to $2 * \text{peak frequency}$. The Nyquist criteria was therefore based on $2 * \text{peak frequency}$.

The area over which to perform the integration is crucial. In terms of a Fresnel zone, the integration zone should be as wide in space as the source is long in time. The "important" low frequency determines the large wavelength for calculating the Fresnel zone width. Typically, a value of $1/2 * \text{peak frequency}$ suffices. (It should be noted that taking advantage of cylindrical symmetry has dictated a rectangular "Fresnel zone", instead of the usual circle.) Therefore, the integration zone width is determined by a minimum frequency, and for a given sub-surface integration area, the surface

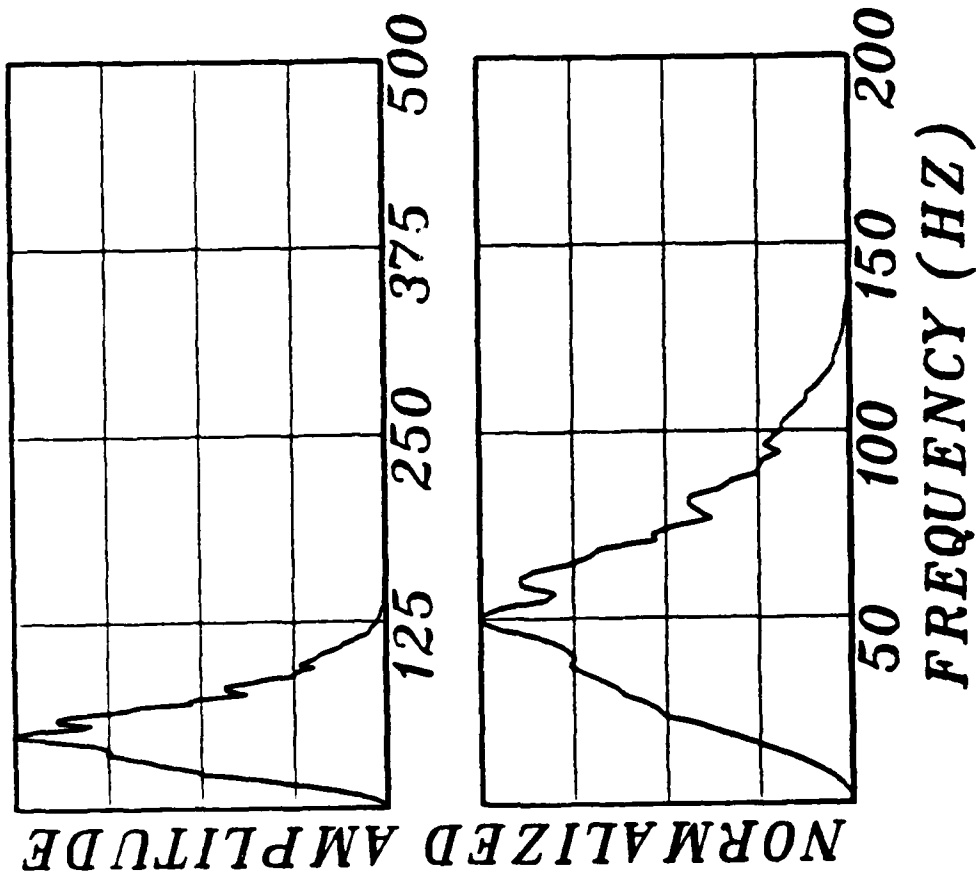
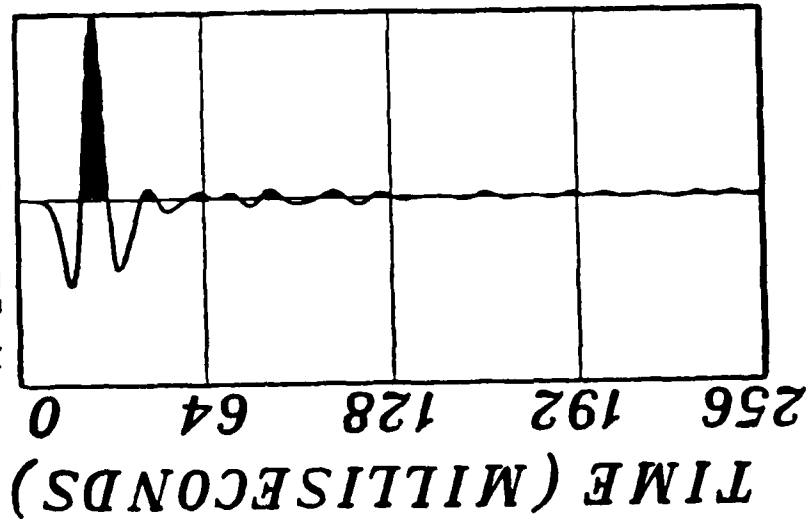
Implementation.

A numerical integration is carried out along the exploding datum employing a constant X increment. If the distance between segments is too large (relative to "important" short wavelengths) aliasing occurs, manifesting itself in the form of very "ringy" late arrivals. A convolutional averaging operator may be applied if desired, and if necessary. If sampling is done properly, the averaging operator automatically reduces to a delta function, and thus has no effect.

For each receiver location a Fresnel zone is calculated, proportional to the longest important wavelength in the source function. The numerical spatial sampling is then determined such that the high frequency content of the late segment contributions are not aliased.

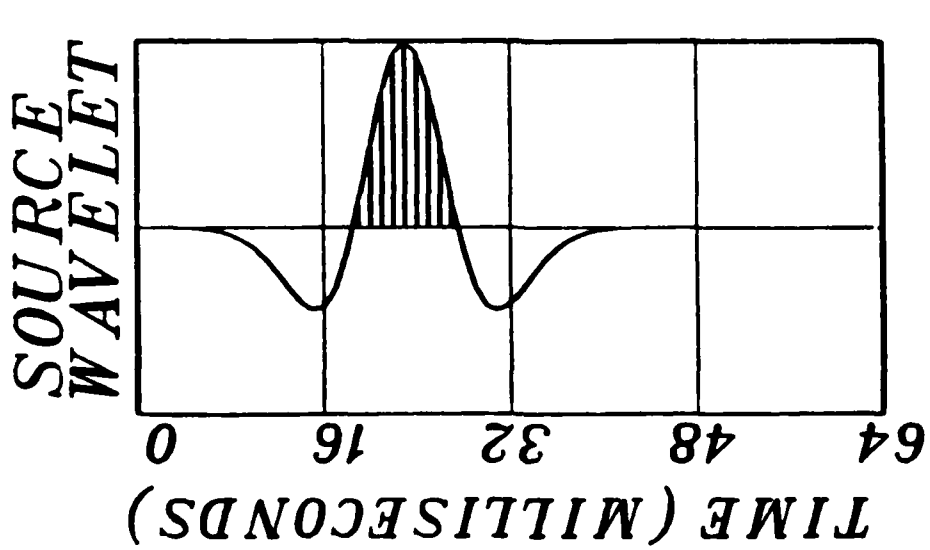
As detailed previously, the recorded response from an exploding plane is obtained by summing responses of exploding lines. Figure 4 illustrates an exploding planar reflector at the $z = 5000$ foot level and a receiver at the $z = 10,000$ foot level. Each line drawn from the plane to the receiver represents a single line source contribution in the plane. The individual contributions before summation are plotted in Figure 5. As long as the spatial sampling is fine enough, when the contributions are added together they should produce a wavelet resembling the Ricker source wavelet. In Figure 6 it is seen that the sampling is adequate for that portion of the surface directly under the receiver location. However, as the distance increases to each segment, so does the travel time, and eventually contributions are arriving too far apart, and aliasing occurs. In the

KIRCHHOFF
WAVELET



MODEL 122

FIGURE 8



MODEL 119

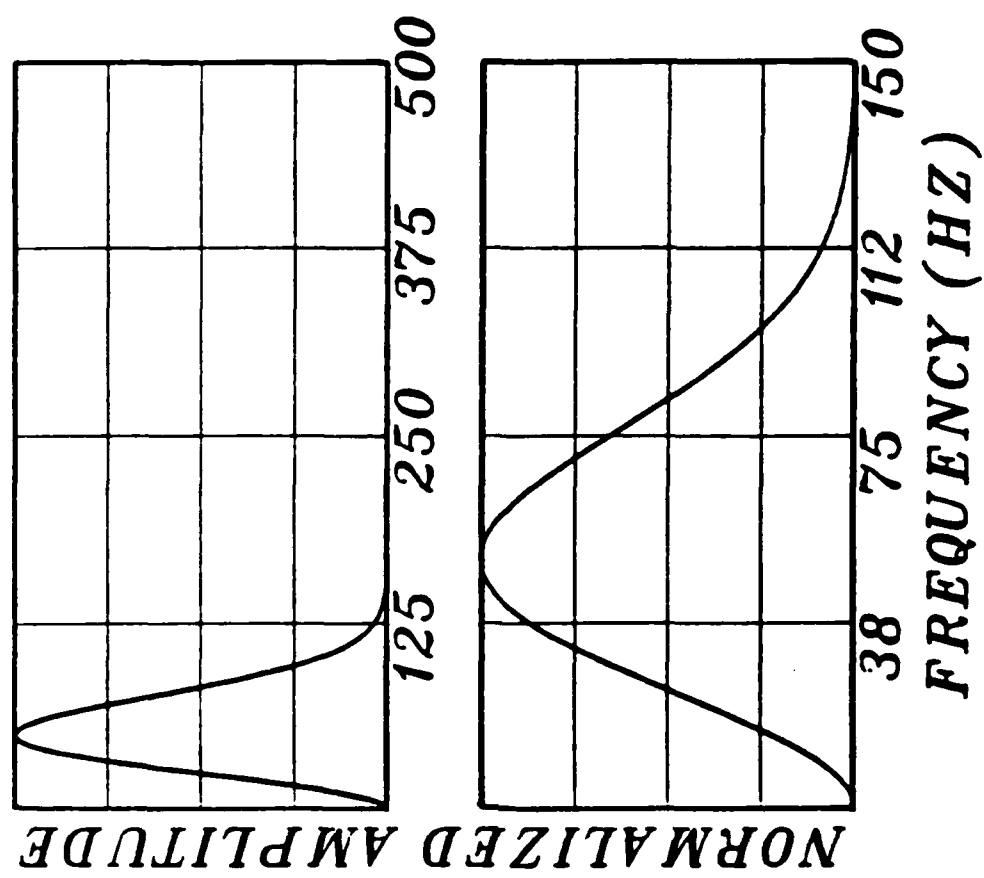


FIGURE 9

KIRCHHOFF INTEGRATION SEGMENTS

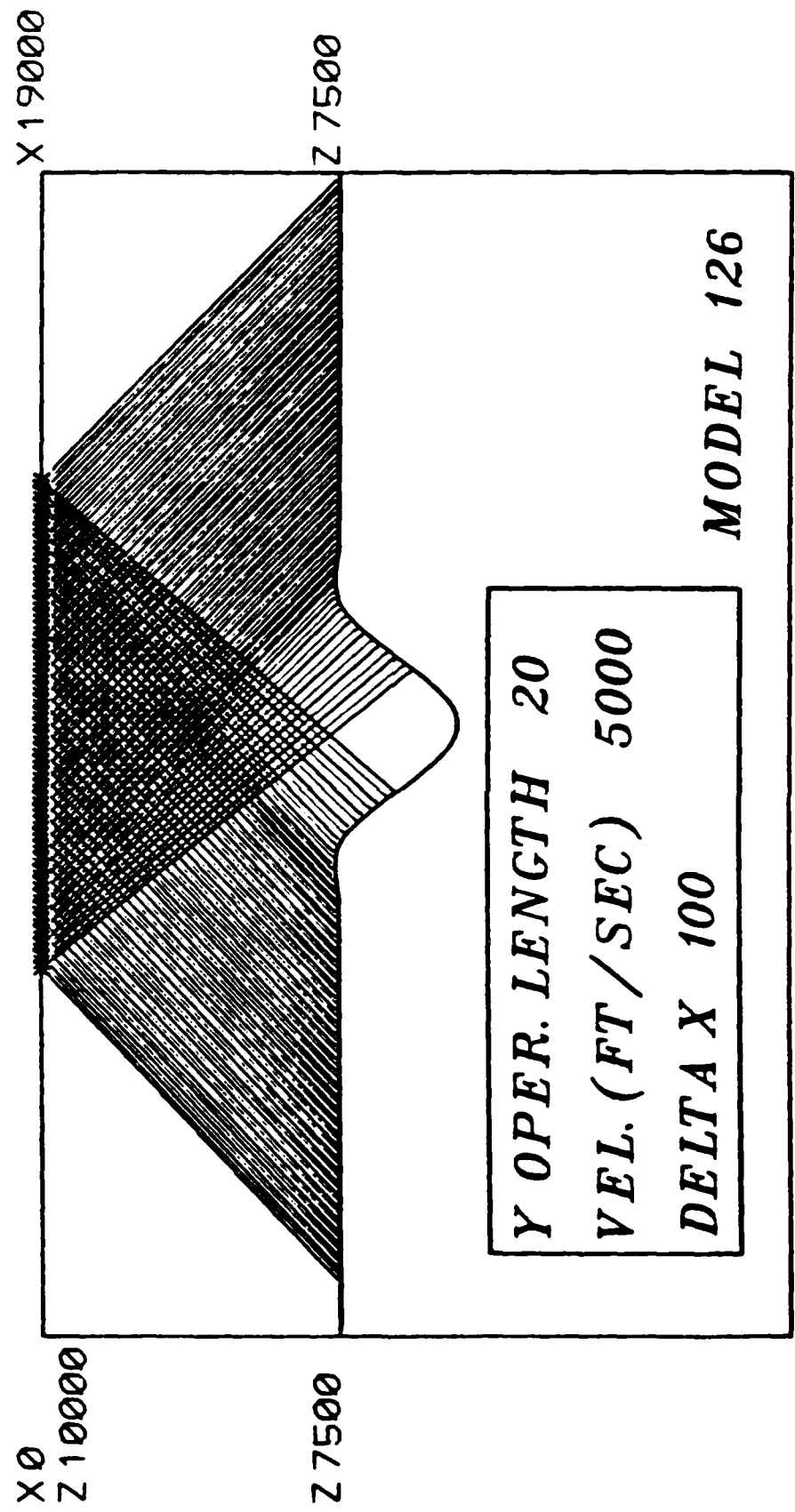
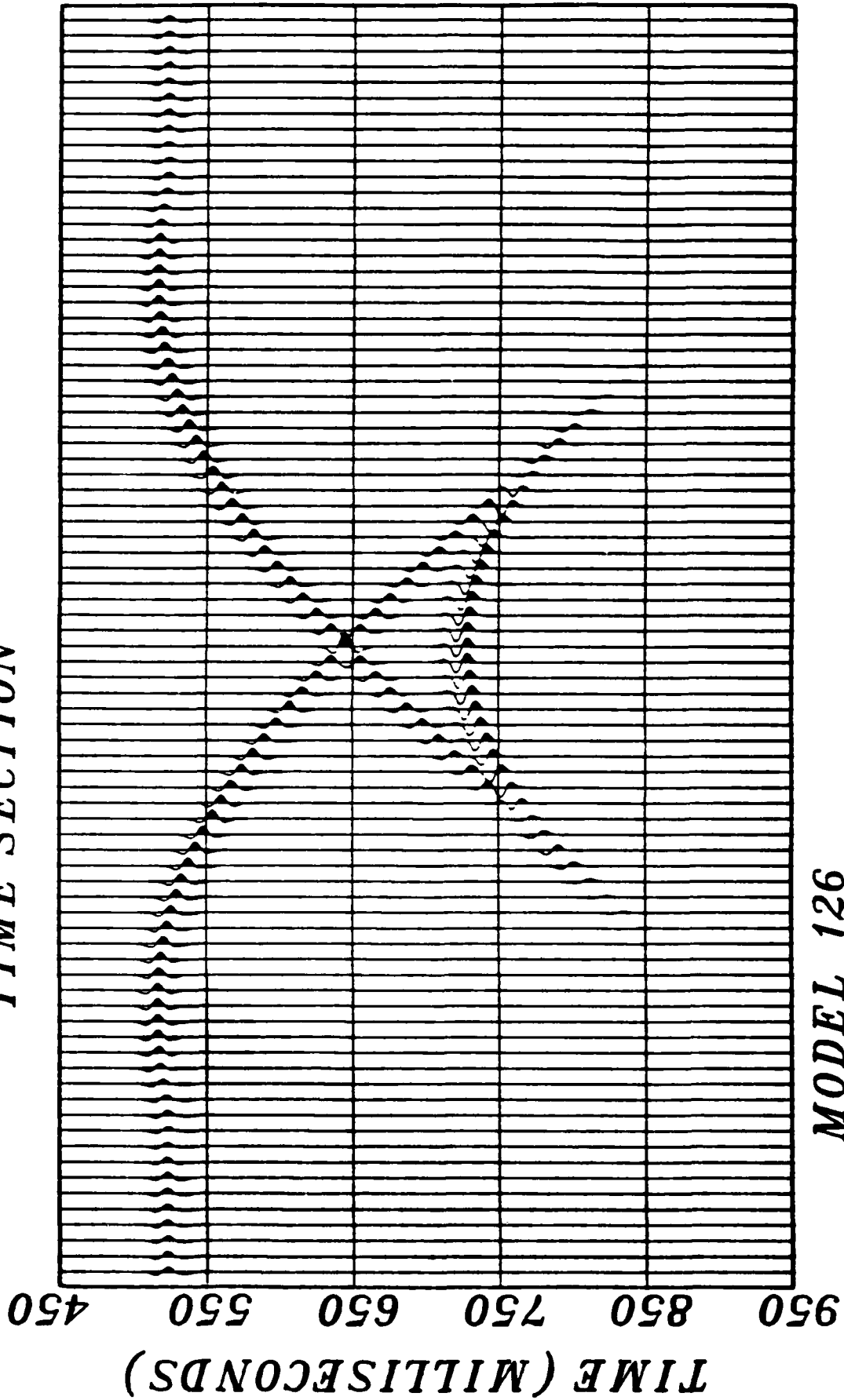


FIGURE 10

TIME SECTION



MODEL 126

FIGURE 11

KIRCHHOFF INTEGRATION SEGMENTS

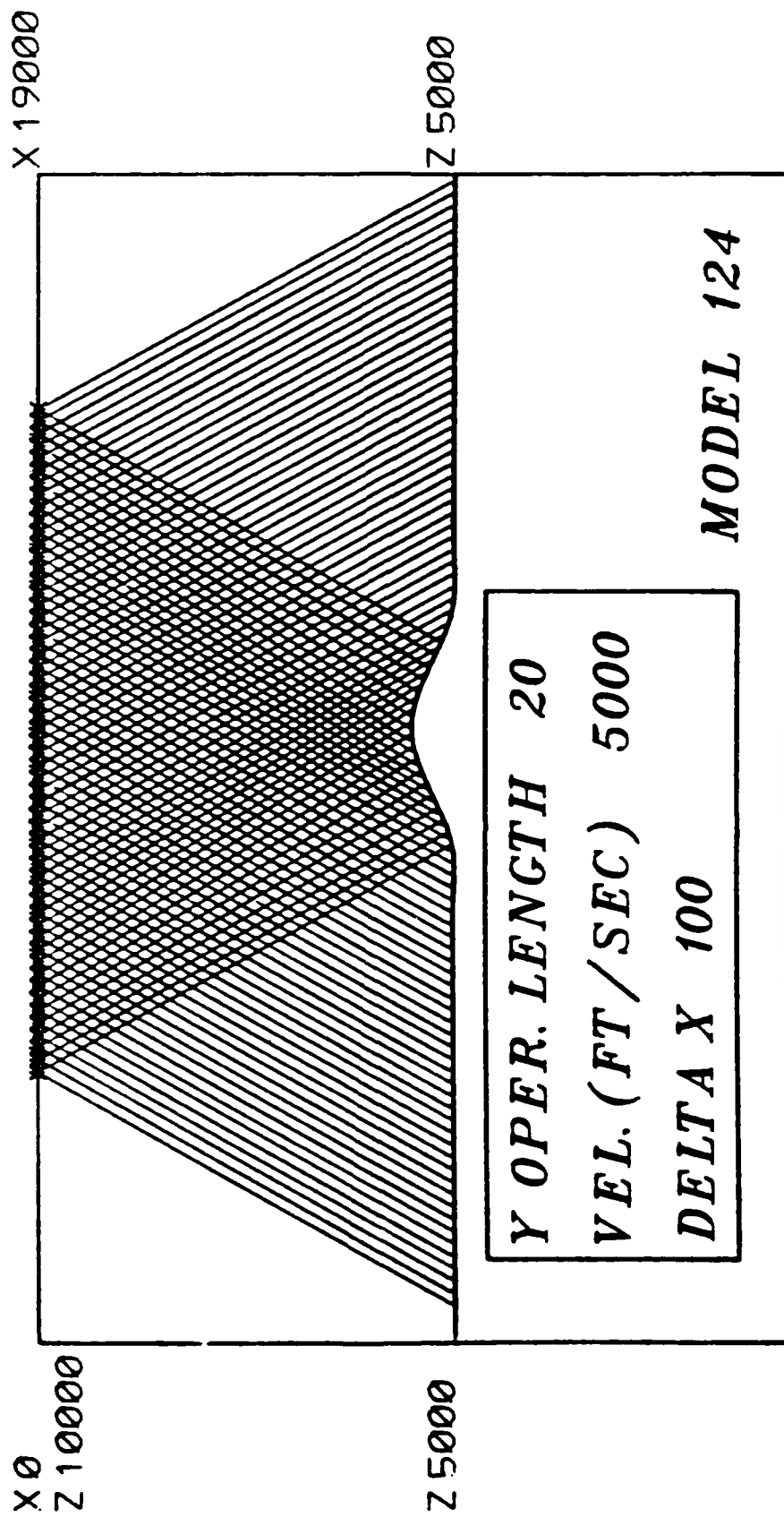
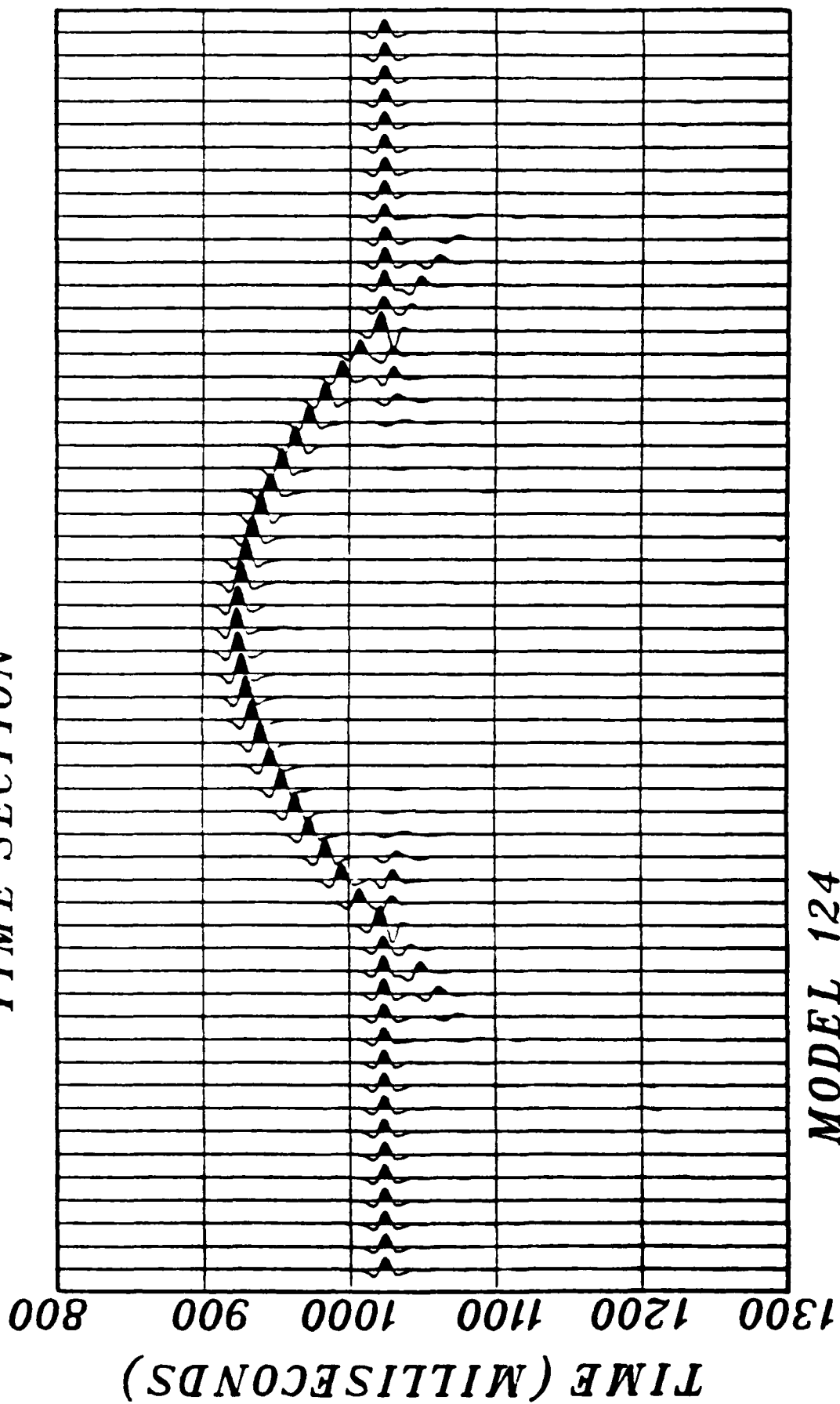


FIGURE 12

TIME SECTION



MODEL 124

FIGURE 13

KIRCHHOFF INTEGRATION SEGMENTS

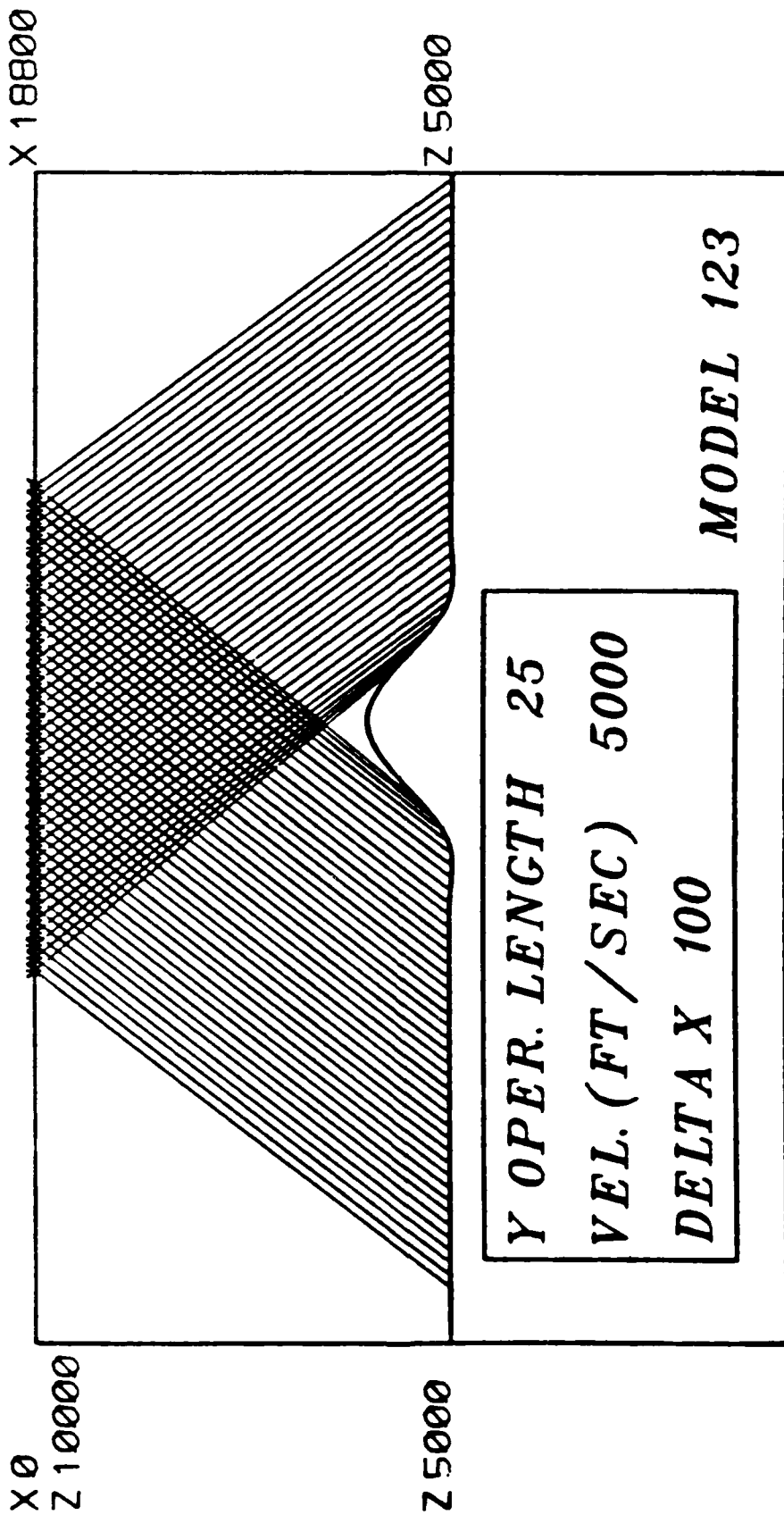
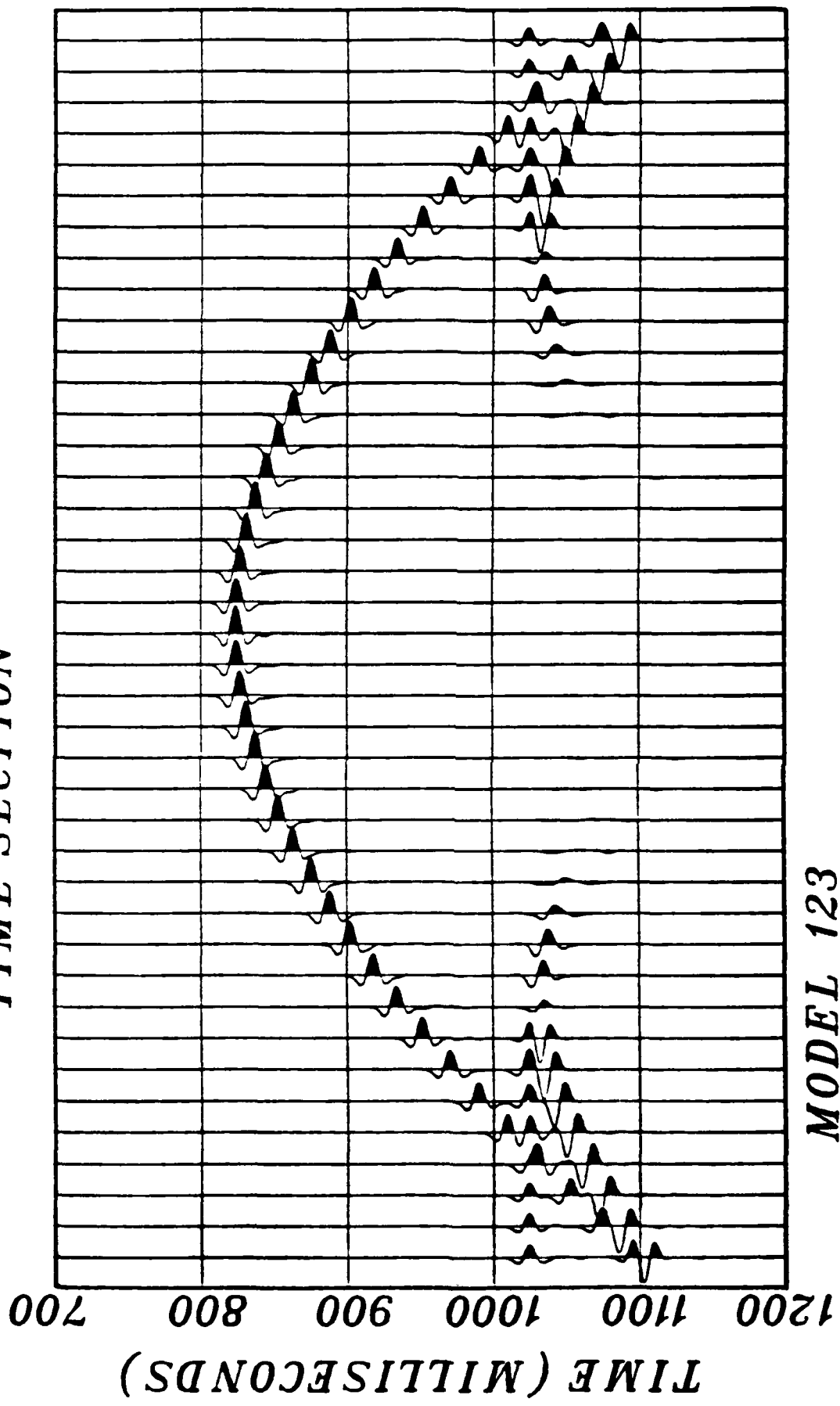


FIGURE 14

TIME SECTION



MODEL 123

FIGURE 15

KIRCHHOFF INTEGRATION SEGMENTS

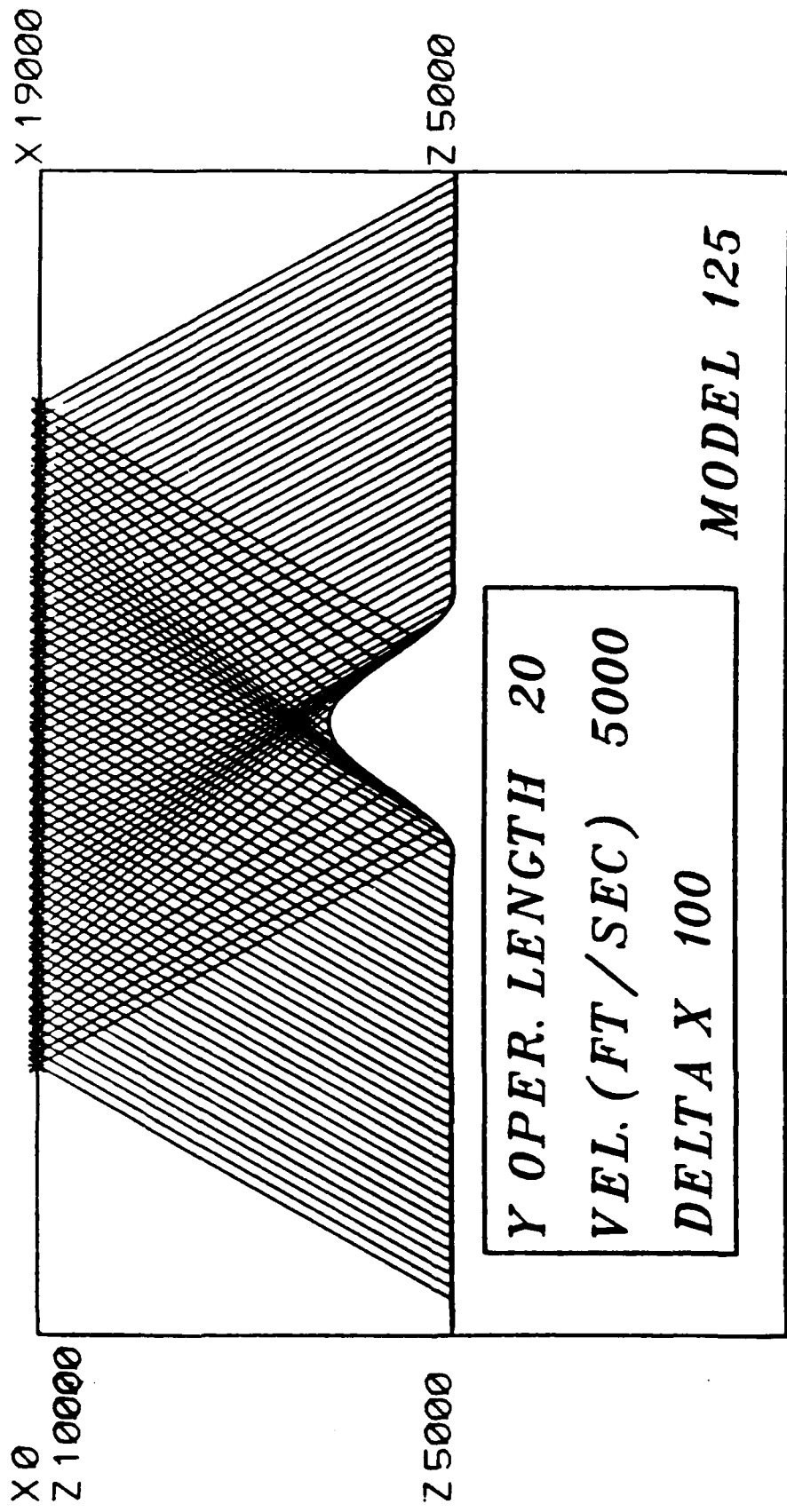


FIGURE 16

TIME SECTION

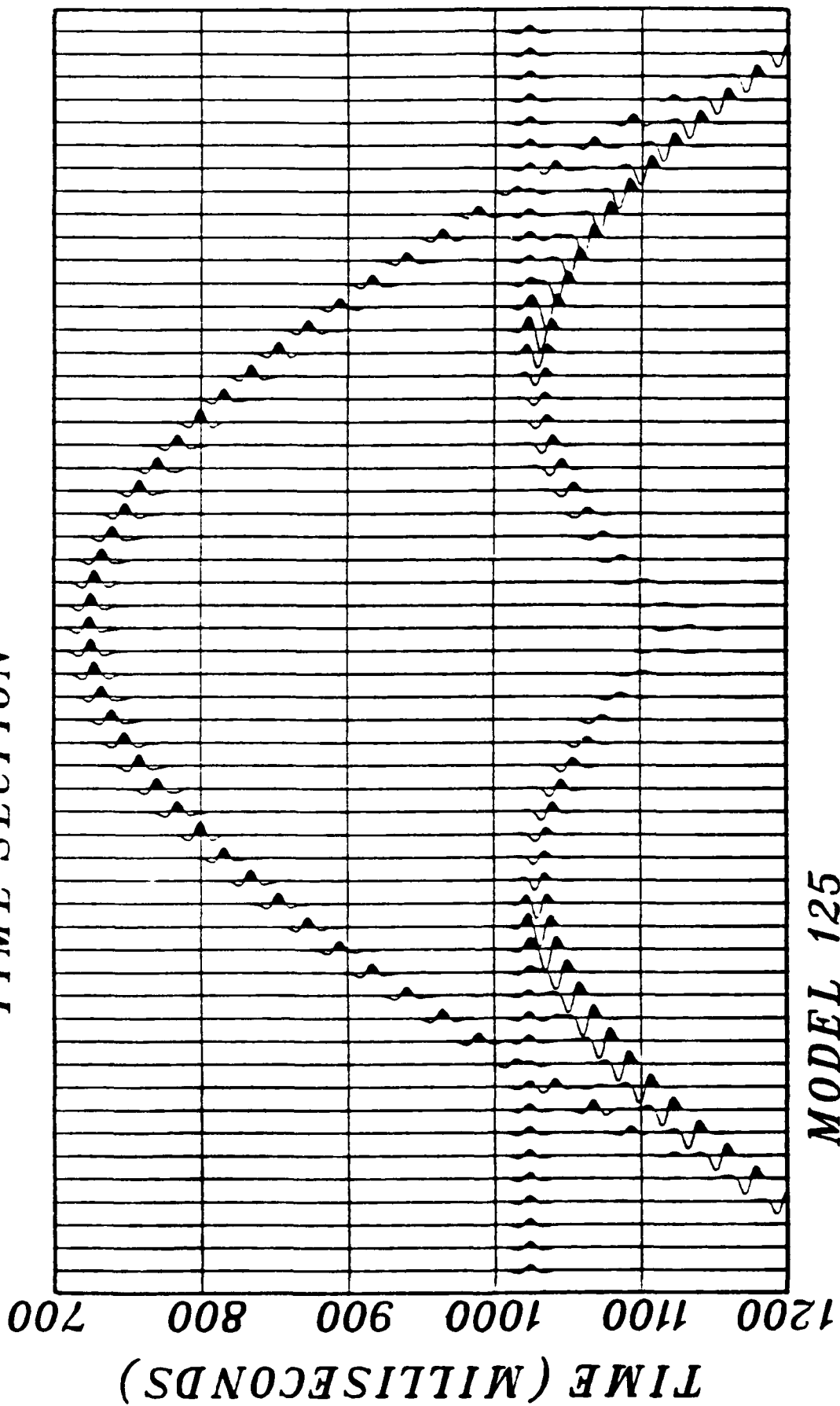


FIGURE 17

REPORT DOCUMENTATION PAGE		READ INSTRUCTIONS BEFORE COMPLETING FORM	
1. REPORT NUMBER CWP-017	2. GOVT ACCESSION NO. AD-A152 349	3. RECIPIENT'S CATALOG NUMBER	
4. TITLE (and Subtitle) Kirchhoff Modeling via Wave Equation Datuming		5. TYPE OF REPORT & PERIOD COVERED Technical	
		6. PERFORMING ORG. REPORT NUMBER	
7. AUTHOR(s) Michael Sullivan		8. CONTRACT OR GRANT NUMBER(s) N00014-84-K-0049	
9. PERFORMING ORGANIZATION NAME AND ADDRESS Center for Wave Phenomena Department of Mathematics Colorado School of Mines, Golden, CO 80401		10. PROGRAM ELEMENT, PROJECT, TASK AREA & WORK UNIT NUMBERS NR SRO-159/84APR20(411)	
11. CONTROLLING OFFICE NAME AND ADDRESS Office of Naval Research Arlington, VA 22217		12. REPORT DATE 1/29/85	
		13. NUMBER OF PAGES 95	
14. MONITORING AGENCY NAME & ADDRESS (if different from Controlling Office)		15. SECURITY CLASS. (of this report)	
		15a. DECLASSIFICATION/DOWNGRADING SCHEDULE	
16. DISTRIBUTION STATEMENT (of this Report) This document has been approved for public release and sale; its distribution is unlimited.			
17. DISTRIBUTION STATEMENT (of the abstract entered in Block 20, if different from Report)			
18. SUPPLEMENTARY NOTES			
19. KEY WORDS (Continue on reverse side if necessary and identify by block number) Kirchhoff Modeling, Wave Equation Datuming, Rayleigh II integral, data continuation, velocity replacement.			
20. ABSTRACT (Continue on reverse side if necessary and identify by block number) see reverse side			

ABSTRACT

The acoustic reflection response of a plane wave on a cylindrical surface is calculated from a specialization of the Kirchhoff integral. Computational advantages are obtained by assuming that structural changes occur only along the direction of data collection. Off-line geologic invariance permits an integral to be replaced by a short convolution operator. The restriction to single interface modeling permits implementation on personal computers. Also, the single layer algorithm provides the framework for a multi-layer code. Details on implementation, example executions, and program listings are included.

... keywords include: ... 72

END

FILMED

5-85

DTIC